

Chandra X-ray and *Gemini* near-infrared observations of the eclipsing msec pulsar SWIFT J1749.4–2807 in quiescence

Peter G. Jonker^{1,2,3}, Manuel A.P. Torres^{1,2}, Danny Steeghs⁴, Deepto Chakrabarty⁵

¹*SRON, Netherlands Institute for Space Research, Sorbonnelaan 2, 3584 CA, Utrecht, The Netherlands*

²*Harvard-Smithsonian Center for Astrophysics, 60 Garden Street, Cambridge, MA 02138, U.S.A.*

³*Department of Astrophysics/IMAPP, Radboud University Nijmegen, PO Box 9010, 6500 GL Nijmegen, the Netherlands*

⁴*Astronomy and Astrophysics, Department of Physics, University of Warwick, Coventry, CV4 7AL*

⁵*Department of Physics and Kavli Institute for Astrophysics and Space Research, Massachusetts Institute of Technology, Cambridge, MA 02139 U.S.A.*

26 August 2024

ABSTRACT

We report on *Chandra* X-ray and *Gemini-North* near-infrared *K*-band observations of the eclipsing accretion-powered millisecond X-ray pulsar SWIFT J1749.4–2807 in quiescence. Using the *Chandra* observation we derive a source position of Right Ascension: 17:49:31.73 and Declination: -28:08:05.08. The position is accurate to $0''.6$ (90 per cent confidence). We find one source at a magnitude $K=18.44\pm 0.03$ with a position fully consistent with the accurate *Chandra* X-ray localisation and a second source at $K=19.2\pm 0.1$ that falls close to the edge of the error circle in the deep *K*-band images. The presence of a few weaker sources as suggested by previous *H*-band observations presented in the literature cannot be ruled out. There is marginal evidence that the brighter of these two sources is variable. Follow-up spectroscopy of this potential counterpart will show if this source is the true counterpart to SWIFT J1749.4–2807. If so, barring the presence of complicating effects such as heating of the mass-donor star, it would allow for the mass of the neutron star to be measured through the measurement of periodic radial velocity variations.

Key words: binaries — X-rays: binaries — X-rays: individual: SWIFT J1749.4–2807 — stars: neutron

1 INTRODUCTION

Neutron stars provide a laboratory to test the behaviour of matter under physical conditions that are unattainable on Earth. The description of the relations between pressure and density of matter under the extreme conditions encountered in neutron stars (the equation of state; EoS) is one of the ultimate goals of the study of neutron stars already for 40 years now.

An excellent way to constrain proposed EoS is by finding massive neutron stars, as each of the EoS predicts a maximum mass for a neutron star above which it will collapse into a black hole (Lattimer & Prakash 2001). Neutron stars more massive than the canonical value of $1.4 M_{\odot}$ can be found in X-ray binaries, as in those systems the neutron stars can accrete a substantial amount of mass from its binary companion. There is strong evidence that millisecond pulsars evolve out of low-mass X-ray binaries (LMXBs), see for instance Wijnands & van der Klis (1998), Chakrabarty & Morgan (1998) and Archibald et al. (2009). Whereas the average mass of neutron stars that accreted

substantially is $1.5\pm 0.2 M_{\odot}$ (Ozel et al. 2012, see also Zhang et al. 2011), there is a sample of millisecond pulsars where high neutron star masses have been measured. For instance, the mass of the neutron star in FIRST J102347.6+003841 has recently been determined to be $1.71\pm 0.16 M_{\odot}$ (Deller et al. 2012) and the millisecond pulsar PSR J0751+1807 has a mass of $2.1\pm 0.2 M_{\odot}$ (Nice et al. 2005). The most accurately measured mass of a massive neutron star is that in PSR J1614–2230. It has a mass of $1.97\pm 0.04 M_{\odot}$ (Demorest et al. 2010). However, the maximum neutron star mass may be higher still. For instance, the best estimate of the Black Widow pulsar mass is $2.40\pm 0.12 M_{\odot}$ (PSR B1957+20; van Kerkwijk et al. 2011), although the systematic uncertainty on this measurement could be larger than the statistical one.

For dynamical mass measurements in LMXBs that host (millisecond) pulsars, pulse timing can directly constrain the orbit of the neutron star and thus its radial velocity semi-amplitude, K_1 . The radial velocity semi-amplitude of the mass donor star, K_2 , can be measured from optical or near-infrared observations. The ratio between K_1 and K_2 yields the ratio between the mass of the companion star

arXiv:1211.1156v1 [astro-ph.HE] 6 Nov 2012

and the neutron star, q . Alternatively, this q can be determined from the rotational broadening of the stellar absorption lines ($v \sin i$). This $v \sin i$ combined with K_2 gives q via $\frac{v \sin i}{K_2} = (1 + q) \frac{0.49q^{2/3}}{0.6q^{2/3} + \ln(1+q^{1/3})}$ (e.g. see Horne et al. 1986). The system inclination can be determined through modelling of the multi-colour optical lightcurves or, in systems with favorable viewing angles such as SWIFT J1749.4–2807 the X-ray eclipse duration can be used to accurately determine the inclination (Horne 1985). As the inclination is constrained by the geometry (Chanan et al. 1976), mass measurements in eclipsing systems are independent of the modelling that lies behind inclinations derived from ellipsoidal variations. In most cases the system has to be in quiescence such that the accretion continuum is suppressed permitting the detection of photospheric absorption features from the mass donor. These absorption features allow one to measure K_2 and $v \sin i$ from optical or near-infrared spectroscopic observations. The eclipse duration together with q gives an accurate measure of the inclination i (Chanan et al. 1976; Horne 1985). q , i and K_2 together give the neutron star mass.

Recently, it was discovered that the transient SWIFT J1749.4–2807 found in 2006 (Schady et al. 2006; see also Wijnands et al. 2009) exhibits pulsations at 518 Hz (Altamirano et al. 2011). Furthermore, the X-ray light curve shows eclipses at the 8.8 hr orbital period (Markwardt & Strohmayer 2010). For the companion star to fill its Roche lobe in the 8.8 hours orbit its mean density would imply a spectral type of a G3 V–G5 V star if the companion is close to the lower main-sequence. Thus, this source holds the promise of allowing for a model-independent neutron star mass determination. From a type I X-ray burst the upper limit to the distance to this source has been determined to be 6.7 ± 1.3 kpc (Wijnands et al. 2009).

The observed interstellar hydrogen column density N_H towards the source is $\approx 3 \times 10^{22} \text{ cm}^{-2}$ (Ferrigno et al. 2011). As it implies about 17 magnitudes of extinction in the V -band (Predehl & Schmitt 1995) it precludes the search of an optical counterpart. Given that the extinction in the K -band is only $\approx 11\%$ of that in the V -band (Cardelli et al. 1989) it allows for the detection of a near-infrared counterpart. D’Avanzo et al. (2011) searched for a near-infrared counterpart in the $1''.6$ *Swift* error circle in the H -band. Given the crowded field, the relatively large uncertainty on the *Swift* X-ray position and the deep observations, D’Avanzo et al. (2011) found more than 40 potential counterparts.

In this Paper we report on a *Chandra* observation of SWIFT J1749.4–2807 in quiescence. This observation provides an accurate localisation. Using this accurate position we investigate our deep *Gemini* K -band observations obtained under excellent natural seeing conditions for the presence of a counterpart to SWIFT J1749.4–2807. Throughout this paper we use the ephemeris of SWIFT J1749.4–2807 given by Altamirano et al. (2011).

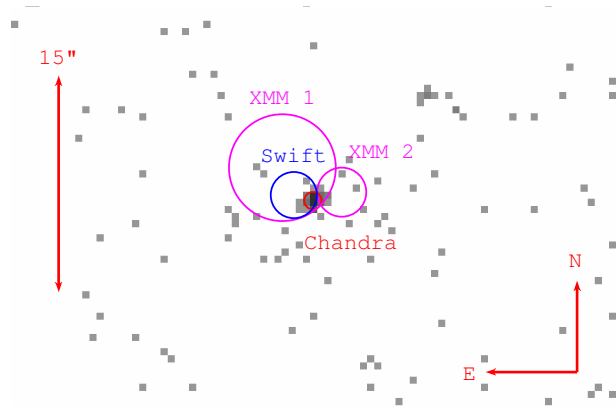


Figure 1. Zoom-in around the *Chandra* ACIS-S3 position of SWIFT J1749.4–2807 (indicated with the small red circle with a radius of $0''.6$). The blue circle indicates the *Swift* (D’Avanzo et al. 2011) position and the magenta circles represent the XMM-*Newton* positions of SWIFT J1749.4–2807 given by Wijnands et al. (2009) (XMM 1) and Degenaar et al. (2012) (XMM 2).

2 OBSERVATIONS, ANALYSIS AND RESULTS

2.1 *Chandra* X-ray observation

We observed SWIFT J1749.4–2807 with the *Chandra* satellite using the back-illuminated S3 CCD-chip of the Advanced CCD Imaging Spectrometer (ACIS) detector (Garmire 1997). The observation started on MJD 56138.09427 (July 30, 2012, 02:15:44 UT) and the on-source exposure time was 24.4 ksec. The observation identification number is 13704.

To mitigate potential pile-up on the off chance that the source was brighter than predicted we windowed the ACIS-S3 CCD such that only half the original CCD size is read out, providing a frame time of 1.54 s of which 0.04 s is used for the CCD read out. We have reprocessed and analysed the data using the *CIAO* 4.3 software employing the calibration files from the Calibration Database version 4.5. In our analysis we have selected events only if their energy falls in the 0.3–7 keV range. All data have been used, as background flaring is very weak or absent.

Since, by design, the source position falls near the optical axis of the telescope (see below), the size of the point spread function is smaller than the ACIS pixel size. Therefore, we follow the method of Li et al. (2004) implemented in the *CIAO* 4.3 tool `ACIS_PROCESS_EVENTS` to improve the image quality of the ACIS data.

Using `WAVDETECT` we detect one X-ray source within the *Swift* (D’Avanzo et al. 2011) and XMM-*Newton* (Wijnands et al. 2009) error circles of SWIFT J1749.4–2807 (see Figure 1). The source is detected $0.2'$ off-axis on the ACIS S3 CCD. The `WAVDETECT` J2000 source position in decimal degrees is: right ascension (RA): 267.38220(2) and declination (Dec): -28.13474(1). The digit in-between brackets denotes the `WAVDETECT` 68 per cent confidence error on RA and Dec. The position in sexagesimal notation is: RA: 17:49:31.73 Dec:-28:08:05.08. The errors given above are due to the error in the source localisation on the CCD alone. The absolute accuracy of the source position is thus determined by the uncertainty in the boresight of the *Chandra* satellite. For sources on the ACIS-S3 CCD this uncertainty is typi-

cally $0.6''$ at 90 per cent confidence. We tried to reduce this boresight uncertainty by investigating if one of the other detected X-ray sources can be safely associated with a source with a well known position but this was not the case.

We have extracted source counts from a circular region of $2''$ radius centered on the source position. Similarly, we have used a circular region with a radius of $50''$ on a source-free region of the CCD to extract background counts. A point-source aperture correction was applied to the auxiliary response file of the source. The net, background subtracted, detected source count rate is 2.9×10^{-3} counts s^{-1} . In total after correcting for the number of expected background photons, 61 source photons have been detected in the energy range between 0.3–7 keV. The number of background photons in the same area in 0.3–7 keV was less than 1.

Using *xspec* version 12.6.0q (Arnaud 1996) we have fitted the spectra of SWIFT J1749.4–2807 using Cash statistics (Cash 1979) modified to account for the subtraction of background counts, the so called W-statistics¹.

Given that we only detected a low number of counts we decided to fix the N_H to 3×10^{22} cm^{-2} in our spectral fits, consistent with the values determined by Ferrigno et al. (2011) and Degenaar et al. (2012). We have used an absorbed powerlaw model fit function to describe the data (the model *pegpwlw* in *xspec*). We visually inspected a plot of the count rate as a function of heliocentric time to search for the presence of the eclipse. The *Chandra* observed count rate is consistent with zero at the predicted heliocentric time of the eclipse. The eclipse duration is consistent with the duration determined by Markwardt & Strohmayer (2010) when the source was in outburst. To account for the fact that the source is eclipsed during 2 ksec (Markwardt & Strohmayer 2010), which is about 8 per cent of the total exposure time, we decrease the effective exposure by 2 ksec when calculating the source flux. We find a best-fit power law index of 0.6 ± 0.4 which gives an unabsorbed X-ray flux of $(0.8 \pm 0.1) \times 10^{-13}$ erg cm^{-2} s^{-1} in the 0.3–7 keV band and 1.4×10^{-13} erg cm^{-2} s^{-1} in the 0.5–10 keV band.

2.2 *Gemini* near-infrared observations

K-band imaging of the field containing SWIFT J1749.4–2807 was performed with the *Gemini-North* telescope on the nights of June 15 and 20, 2012 under observing program GN-2012A-Q-67. The Near Infrared Imaging and Spectrometer (NIRI; Hodapp et al. 2003) instrument was used with the *f/14* camera to yield a field of view of $51'' \times 51''$ with a plate scale of $0''.05$ pixel⁻¹.

The field of SWIFT J1749.4–2807 is crowded and care was taken to avoid as much as possible image artifacts due to saturated stars. In particular, we exclude from the NIRI FOV the *K* ~ 8.6 star 2MASS J17493218–2807563. Therefore, we both rotated the instrument 45 degrees and used a ($p, q=x, 0$)-dithering pattern. Integration times were 10 s in order to mitigate saturation effects from other bright stars in the field of view. Thus the observing sequences consisted of a 5-point dither pattern with offset steps p of 0, 10, -5, 5 and $15''$ and we added three 10 s exposures at each dither

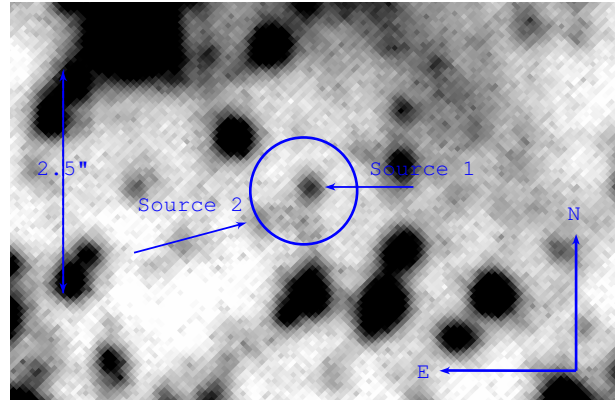


Figure 2. *Gemini-NIRI K* band finder chart obtained from combining those images with seeing better than $0''.31$ on June 15, 2012. The $0''.6$ *Chandra* 90 per cent confidence error circle on the X-ray source position is indicated (circle). We mark source 1 and 2, where the position of source 1 is consistent with the X-ray position. Source 1 shows marginal evidence for variability (at the 4σ level) between the observations of June 15 and June 20, 2012.

position. This pattern was repeated twenty one times yielding a total of 52.5 min on source. The image quality varied during the observations due to the weather conditions. We measure a point-spread function full-width at half maximum (FWHM) between $0''.22$ – $0''.36$ and $0''.23$ – $0''.58$ with a median value of $0''.29 \pm 0''.03$ and $0''.40 \pm 0''.07$ on June 15 and 20, respectively.

The data were processed using both PYTHON scripts and IRAF² tasks developed and provided by the *Gemini* Observatory. Note that sky frames were not subtracted from the data. The observed field is too crowded to allow us to build a useful sky frame from the dithered images and there were no nearby regions on the sky suitable to measure the local sky background.

For the analysis, we generated images by stacking all the reduced frames using *imcoadd*. In this way we obtained for the night of June 15 seven combined images of 150 s on source each. We also combined the images with seeing $< 0''.31$ of the first night into one average image. The night of June 20 was of less good image quality (see above) and a single combined frame was built totalling 1770 s on source.

We improved the astrometry of the best-seeing frame using the position of six 2MASS stars that were well separated from other stars and which did not saturate the *Gemini* NIRI detector. A fit of pixel scale in x and y , and orientation provide an root-mean-square (rms) uncertainty of $0''.03$ for a pixel scale of $0''.05$ per pixel in x and y and an orientation of 44.9° .

In Fig. 2 we show the finding chart of the field of SWIFT J1749.4–2807 using the best seeing image of June 15. Overplotted is the 90 per cent confidence error circle on the *Chandra* X-ray position of the source. A clear source is detected near the centre of the error circle (star 1) and towards the south-east corner just outside the formal 90 per cent confidence error circle, lies another fainter potential candidate counterpart (star 2).

¹ see <http://heasarc.gsfc.nasa.gov/docs/xanadu/xspec/manual/>

² IRAF is distributed by the National Optical Astronomy Observatories

We performed aperture photometry on the images using DAOPHOT in IRAF to compute the instrumental magnitudes for the objects of interest. Absolute flux calibration of the images was obtained selecting isolated stars with magnitudes reported in the UKIDSS-DR6 Galactic Plane Survey (UGPS; Lucas et al. 2008). Both the NIRI and the UKIDSS photometric systems are close representations of the Mauna Kea Observatory (MKO) standard system. Differential photometry was obtained on each of the averaged images to derive the flux variability of the sources as a function of time. The photometric results given here are with respect to the star UGPS J176971.32–288889.6 ($K = 14.551 \pm 0.022$). The scatter in the light curves build for this UGPS star using other bright and isolated comparison stars shows that the differential photometry is accurate to $\lesssim 1$ per cent.

Photometry of the two candidate counterparts on the combined best seeing image of June 15, 2012, yields a magnitude of $K_1 = 18.44 \pm 0.03$ and $K_2 = 19.20 \pm 0.06$ for star 1 and star 2, respectively. The magnitude during the observation on June 20, 2012 is $K_1 = 18.75 \pm 0.07$ and $K_2 = 19.3 \pm 0.1$ mag. So, with an average magnitude of $K_1 = 18.44 \pm 0.03$ on June 15, and $K_1 = 18.75 \pm 0.07$ on June 20, 2012, there is evidence at the 4σ level that this source is variable.

3 DISCUSSION

Using *Chandra* we obtained a 24.4 ksec exposure of the eclipsing msec. pulsar SWIFT J1749.4–2807 in quiescence. We detected the source at an unabsorbed flux of 2×10^{-13} erg cm^{-2} s^{-1} in the 0.5–10 keV band and we provide a position accurate to $0''.6$ at 90 per cent confidence. At a distance upper limit of 6.7 ± 1.3 kpc (Wijnands et al. 2009), this flux corresponds to an X-ray luminosity of 1×10^{33} erg s^{-1} in the 0.5–10 keV band. Owing to the uncertainty in the high hydrogen column density towards the source this number is uncertain, but the value is consistent with that found before from XMM-*Newton* observations in quiescence (Wijnands et al. 2009; Degenaar et al. 2012). The derived quiescent X-ray luminosity is also in agreement with the rough correlation between quiescent X-ray luminosity and the orbital period, although the source is on the bright end of the observed correlation (a plot highlighting this correlation can be found in Rea et al. 2011). The best-fit power law index of the X-ray spectrum is 0.6 ± 0.4 , which is steep for quiescent neutron stars, however, the uncertainty on this number is currently such that it could be made consistent with more canonical values of 1.5–2 particularly if N_{H} is somewhat higher than the 3×10^{22} cm^{-2} that was used in the fit (see for instance the powerlaw fit in Degenaar et al. 2012).

In addition to the *Chandra* observation, we obtained *Gemini* K -band images under excellent natural seeing conditions of the field of SWIFT J1749.4–2807. The position of one point source is consistent with the X-ray location and a second is bordering the *Chandra* error circle. There is marginal evidence for the brighter of the two to be variable. The observed interstellar hydrogen column density, N_{H} , towards SWIFT J1749.4–2807 is $\approx 3 \times 10^{22}$ cm^{-2} (Ferrigno et al. 2011). This yields an extinction in the K -band of 1.9 mag (Cardelli et al. 1989). However, as $A_{\text{V}}/E(B - V) = R_{\text{V}}$ is known to be closer to 2.5 than 3.1 for fields towards the

bulge (Nataf et al. 2012) this implies that A_{K} would be 1.7 mag for $R_{\text{V}}=2.5$.

For the companion star to fill its Roche lobe in the 8.8 hours orbit its mean density would imply a spectral type of a G3 V–G5 V star if the companion is close to the lower main-sequence. Note that the spectral type of G5 V that we derive here is consistent with the broad mass range for the companion star (0.45–0.8 M_{\odot}) that is derived by Markwardt & Strohmayer (2010) and Altamirano et al. (2011) as the mass donors in LMXBs and CVs are often under-massive for their spectral type (Knigge et al. 2011). For a G5 V donor star, the absolute magnitude in the V - and in the K -band is $M_{\text{V}} = 5.1$ and $M_{\text{K}} = 3.5$, respectively (see Cox 2000 and Tokunaga 2000, respectively). At a distance upper limit of 6.7 kpc the distance modulus, DM, is 14.1. Allowing for 1.7 magnitudes of extinction in the K -band will mean that the companion star has an apparent magnitude of $m_{\text{K}} = \text{DM} + 1.7 + M_{\text{K}}$ yielding $m_{\text{K}} = 19.3$ for the G5 V star. The observed K band magnitude of ~ 18.6 is consistent with this if the source is more nearby than the 6.7 kpc upper limit (i.e. the source has to be at ~ 5 kpc) and/or if the extinction in the K -band is lower than 1.7 magnitudes. The latter can be the case if part of the observed N_{H} is due to ionised material for instance material local to the source.

Previous to our work, D’Avanzo et al. (2011) obtained H -band adaptive optics observations with the Very Large Telescope. Of the 41 sources that those authors detected inside the error circle of the *Swift* X-ray position, five fall inside the *Chandra* error circle; six if we include our source 2. Two of these six sources coincide with the position of the two potential counterparts that we found. In Table 1 we list the properties found by D’Avanzo et al. (2011) for these six sources.

Our star 1 at RA: 17:49:31.73 Dec: -28:08:05.09 would correspond to source number 8 in table 2 of D’Avanzo et al. (2011) (see Table 1). Our star 2 which is at RA: 17:49:31.768 Dec: -28:08:05.41 would correspond to their entry number 24. The other four sources inside the *Chandra* error circle are not significantly detected in our *Gemini* data, although there is some evidence for additional flux to the south of star 1, which could be caused by either source 25 or source 27, or by both sources together.

The extinction towards SWIFT J1749.4–2807 in the H -band is ~ 1.2 mag more than that in the K -band. The $(H - K)_0$ colour of A–M5 stars is between 0 and 0.3 mag (Tokunaga 2000). Therefore, the magnitudes of the two sources that we find should be, at most, 1.5 magnitude brighter than the H -band magnitudes reported in D’Avanzo et al. (2011) for these two sources. However, comparing our observed K band magnitudes with the H -band magnitudes reported by D’Avanzo et al. (2011) (see Table 1) we see that the observed $H - K$ colour is approximately 2.4 magnitudes for star 1 and 2.8 magnitudes for star 2. We investigated the potential reason for this peculiar colour by comparing our magnitudes as well as the H -band magnitudes derived by D’Avanzo et al. (2011) with the magnitudes of 2MASS and UKIDSS stars in the images. The H -band magnitude of the star at RA: 17:49:31.88 Dec: -28:08:03.3 reported by D’Avanzo et al. (2011) (entry number 1 in their paper) is 16.26, however it has $H = 15.01 \pm 0.05$ according to the UKIDSS database, this is nearly 1.3 magnitudes brighter. In addition, we looked up the H and K magnitudes reported

Table 1. Position and H -band magnitudes from D’Avanzo et al. (2011) for the sources close to the *Chandra* 90 per cent confidence error circle. The offset of the position of each of the stars with respect to the centre of the *Chandra* position as well as the K -band magnitudes from this work are given. Note that the H -band magnitudes from D’Avanzo et al. (2011) are off; approximately -1.3 has to be added to the reported magnitudes (see Discussion).

RA	Dec	Src #	H -band mag	H -band mag	Offset	K -band
		D’Avanzo et al. 2011	Aug 30, 2010	Aug 31, 2011	"	mag
17:49:31.730	-28:08:04.50	32	22.75±0.11	22.66±0.09	0.58	–
17:49:31.76	-28:08:05.39	41	23.99±0.35	22.68±0.09	0.53	–
17:49:31.720	-28:08:05.50	25	22.22±0.07	21.86±0.07	0.44	–
17:49:31.730	-28:08:05.40	27	22.54±0.08	22.38±0.08	0.32	–
17:49:31.72	-28:08:05.1	8	20.81±0.05	20.74±0.05	0.11	18.44±0.03 (src 1)
17:49:31.77	-28:08:05.4	24	22.20±0.08	21.94±0.12	0.64	19.20±0.06 (src 2)

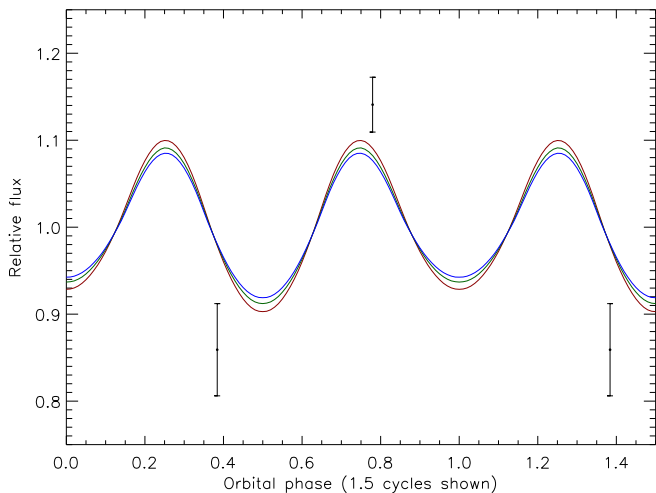


Figure 3. The expected ellipsoidal variations for a Roche lobe filling G5V star with in decreasing order of amplitude a mass ratio of $q = 0.3, 0.5, 0.7$. The magnitudes for source 1 on the night of June 15, 2012 (near phase 0.77) and June 20, 2012 (near phase 0.36) are overplotted, showing that the observed variability has the right sign in the sense that the source is brighter near phase 0.77 than near phase 0.36. Changes in the predicted ellipsoidal modulations for a K0 V star are marginal with respect to those of the G5 V star shown.

in the VISTA (Visible and Infrared Survey Telescope for Astronomy) variable sources in the Via Lactea (VVV) survey (Minniti et al. 2010, Catelan et al. 2011) and the bright star has $H=14.9$, so close to the value provided by UKIDSS. We conclude that the photometric calibration presented in D’Avanzo et al. (2011) is off by 1.3 magnitudes. Indeed, correcting for this photometric offset would imply observed $H - K$ colours of our stars 1 and 2 in line with what is expected given the extinction towards the source. The alternative scenarios that could potentially explain the observed $H - K$ colours, such as a significantly higher extinction or a more shallow extinction law (a large value of R_V) are not likely nor necessary to explain the $H - K$ colours.

As a next step, spectroscopic follow-up is suggested to confirm/reject source 1 as the counterpart. Spectra should show typical late type star absorption features that should move as a function of the orbital phase of SWIFT J1749.4–2807. Typical features in the K -band spectra of late type

stars are the CO band head absorption bands (e.g. Greiner et al. 2001b; Greiner et al. 2001a). If confirmed, source 1 is within reach of current instrumentation for time-resolved dynamical studies. If source 1 is found not to be the counterpart, potentially, one can search for the right counterpart by using adaptive optics observations under photometric conditions. However, given that the maximum amplitude (peak-to-peak) of ellipsoidal variations is 0.2 magnitudes for a mass ratio of $q = 0.3$ this is challenging. In Figure 3 we plot the magnitudes of source 1 over the expected ellipsoidal variations for a Roche lobe filling companion star of spectral type G5V for three different values of q . With decreasing amplitude of the modulations we plot $q = 0.3, 0.5, 0.7$. The figure shows that the observed variability has the right sign given that the source is brighter near phase 0.77 than near phase 0.36. For smaller mass ratios the peak-to-peak amplitude increases, which given that the two data points lie above and below the curves, could hint at a more extreme mass ratio. Such a mass ratio could be accommodated by a neutron star more massive than $1.4 M_\odot$ and a mass donor star under-massive for its spectral type. Furthermore, if light from a residual accretion disc is present it will reduce the apparent amplitude of the ellipsoidal modulations. Thus, adding a significant amount of light of an accretion disc to the model can only be made in agreement with the two data points for a (very) small mass ratio q . Potentially, if the neutron star heats the companion star one can find variations due to changes in the aspect of the companion star (see for instance Homer et al. 2001; Burderi et al. 2003; Jonker et al. 2008; D’Avanzo et al. 2009). However, such variations would possibly be larger than the ellipsoidal variations and they would produce a bright K -band magnitude at orbital phase of 0.5 and this is not seen in the current data (see Figure 3). Given that the orbital period of SWIFT J1749.4–2807 is larger than that of the accretion powered millisecond pulsars where this effect has been found before, the amplitude of the effect will be reduced. Finally, flickering often observed in optical and near-infrared light of X-ray binaries in quiescence due to for instance short-term variations of the accretion disc can also explain the observed variability (e.g. see Reynolds et al. 2008; Cantrell et al. 2010).

ACKNOWLEDGMENTS

The authors acknowledge the referee for providing useful comments that helped improve the manuscript. PGJ ac-

knowledges support from a VIDI grant from the Netherlands Organisation for Scientific Research. PGJ acknowledges Theo van Grunsven for discussions on the amplitude of the ellipsoidal variations and for producing Figure 3. MAPT and PGJ acknowledge Knut Olsen for discussions on the NIRI data reduction. This research has made use of data obtained from the Chandra Source Catalog, provided by the Chandra X-ray Center (CXC) as part of the Chandra Data Archive (ADS/Sa.CXO#CSC).

REFERENCES

- Altamirano, D., et al., 2011, *ApJ*, 727, L18
 Archibald, A. M., et al., 2009, *Science*, 324, 1411
 Arnaud, K. A., 1996, in *ASP Conf. Ser. 101: Astronomical Data Analysis Software and Systems V*, vol. 5, p. 17
 Burderi, L., Di Salvo, T., D’Antona, F., Robba, N. R., Testa, V., 2003, *A&A*, 404, L43
 Cantrell, A. G., et al., 2010, *ApJ*, 710, 1127
 Cardelli, J. A., Clayton, G. C., Mathis, J. S., 1989, *ApJ*, 345, 245
 Cash, W., 1979, *ApJ*, 228, 939
 Catelan, M., et al., 2011, in *McWilliam, A., ed., RR Lyrae Stars, Metal-Poor Stars, and the Galaxy*, p. 145
 Chakrabarty, D., Morgan, E. H., 1998, *Nat*, 394, 346
 Chanan, G. A., Middleditch, J., Nelson, J. E., 1976, *ApJ*, 208, 512
 Cox, A. N., 2000, *Allen’s astrophysical quantities, Allen’s astrophysical quantities*, 4th ed. Publisher: New York: AIP Press; Springer, 2000. Edited by Arthur N. Cox. ISBN: 0387987460
 D’Avanzo, P., Campana, S., Casares, J., Covino, S., Israel, G. L., Stella, L., 2009, *A&A*, 508, 297
 D’Avanzo, P., Campana, S., Muñoz-Darias, T., Belloni, T., Bozzo, E., Falanga, M., Stella, L., 2011, *A&A*, 534, A92
 Degenaar, N., Patruno, A., Wijnands, R., 2012, *ApJ*, 756, 148
 Deller, A. T., et al., 2012, *ArXiv e-prints*
 Demorest, P. B., Pennucci, T., Ransom, S. M., Roberts, M. S. E., Hessels, J. W. T., 2010, *Nat*, 467, 1081
 Ferrigno, C., et al., 2011, *A&A*, 525, A48
 Garmire, G. P., 1997, in *Bulletin of the American Astronomical Society*, vol. 29 of *Bulletin of the American Astronomical Society*, p. 823
 Greiner, J., Cuby, J. G., McCaughrean, M. J., 2001a, *Nat*, 414, 522
 Greiner, J., Cuby, J. G., McCaughrean, M. J., Castro-Tirado, A. J., Mennickent, R. E., 2001b, *A&A*, 373, L37
 Hodapp, K. W., et al., 2003, *PASP*, 115, 1388
 Homer, L., Charles, P. A., Chakrabarty, D., van Zyl, L., 2001, *MNRAS*, 325, 1471
 Horne, K., 1985, *MNRAS*, 213, 129
 Horne, K., Wade, R. A., Szkody, P., 1986, *MNRAS*, 219, 791
 Jonker, P. G., Torres, M. A. P., Steeghs, D., 2008, *ApJ*, 680, 615
 Knigge, C., Baraffe, I., Patterson, J., 2011, *ApJS*, 194, 28
 Lattimer, J. M., Prakash, M., 2001, *ApJ*, 550, 426
 Li, J., Kastner, J. H., Prigozhin, G. Y., Schulz, N. S., Feigelson, E. D., Getman, K. V., 2004, *ApJ*, 610, 1204
 Lucas, P. W., et al., 2008, *MNRAS*, 391, 136
 Markwardt, C. B., Strohmayer, T. E., 2010, *ApJ*, 717, L149
 Mignani, D., et al., 2010, *New Astronomy*, 15, 433
 Nataf, D. M., et al., 2012, *ArXiv e-prints*
 Nice, D. J., Splaver, E. M., Stairs, I. H., Löhmer, O., Jessner, A., Kramer, M., Cordes, J. M., 2005, *ApJ*, 634, 1242
 Ozel, F., Psaltis, D., Narayan, R., Santos Villarreal, A., 2012, *ArXiv e-prints*
 Predehl, P., Schmitt, J. H. M. M., 1995, *A&A*, 293, 889
 Rea, N., Jonker, P. G., Nelemans, G., Pons, J. A., Kasliwal, M. M., Kulkarni, S. R., Wijnands, R., 2011, *ApJ*, 729, L21
 Reynolds, M. T., Callanan, P. J., Robinson, E. L., Froning, C. S., 2008, *MNRAS*, 387, 788
 Schady, P., Beardmore, A. P., Marshall, F. E., Palmer, D. M., Rol, E., Sato, G., 2006, *GRB Coordinates Network*, 5200, 1
 Tokunaga, A. T., 2000, *Infrared Astronomy*, p. 143
 van Kerkwijk, M. H., Breton, R. P., Kulkarni, S. R., 2011, *ApJ*, 728, 95
 Wijnands, R., van der Klis, M., 1998, *Nat*, 394, 344
 Wijnands, R., Rol, E., Cackett, E., Starling, R. L. C., Remillard, R. A., 2009, *MNRAS*, 393, 126
 Zhang, C. M., et al., 2011, *A&A*, 527, A83